Rare Metal Materials and Engineering
Volume 49, Issue 1, January 2020
Available online at www.rmme.ac.cn

Science Press

Cite this article as: Rare Metal Materials and Engineering, 2020, 49(1): 0021-0026.

ARTICLE

Evolution of Microstructure and Formability of AZ31 Mg Alloy Sheets Processed by Continuous Bending with Various Accumulated Strains

Han Tingzhuang[1], Huang Guangsheng[2], Wang Lifei[3], Jiang Bin[2], Wang Guangang[2], Tang Aitao[2], Pan Fusheng[2]

[1] Heavy Machinery Engineering Research Center of the Ministry of Education, Taiyuan University of Science and Technology, Taiyuan 030024, China; [2] State Key Laboratory of Mechanical Transmission, Chongqing University, Chongqing 400044, China; [3] Taiyuan University of Technology, Taiyuan 030024, China

Abstract: AZ31 alloy sheets were subjected to continuous bending (CB) process with various accumulated strains in a single pass at room temperature, followed by annealing treatment. The corresponding microstructure and mechanical properties of as-received and CB sheets were investigated. The results indicate that no twins are observed in all microstructures during the CB process. Abnormal grain growth occurs in the surface part after annealing and the depth of coarse-grained layer increases with increasing the accumulated strain. Moreover, the CB sheets in annealing condition exhibit a RD-tilt basal texture, and the inclination angle increases with increasing the accumulated strain. Compared to the as-received sample with a strong basal texture, the CB processed samples exhibit better stretch formability (cupping test value increases from 2.3 mm to 4.9 mm, increased by ~113%), due to smaller *r*-value and larger *n*-value which are related to the texture evolution.

Key words: magnesium alloy; continuous bending; microstructure; texture; mechanical properties; formability

Due to the low density, high specific strength and high specific stiffness, magnesium alloys have a significant potential in wide range of industrial applications, including transport vehicles, electronics and aerospace industries [1-3]. However, for magnesium alloys with the hexagonal close-packed (hcp) crystalline structure, a limited number of slip systems may be activated during plastic deformation, which can hardly offer an arbitrary shape change at the grain level[4,5]. Moreover, conventionally rolled and extruded sheets usually exhibit a strong basal texture with the basal planes parallel to the rolling direction, resulting in a great planar anisotropy. This results in a bad deformability in the thickness direction and a stronger anisotropy [6-8]. Therefore, magnesium alloy sheets usually exhibit low ductility and formability at ambient temperature, restricting their wide industrial application. And how to improve the stretch formability of Mg alloy sheets is of great importance. Recently, the texture control has been considered as an effective way for improving the formability, and many processing techniques such as cross-roll rolling (CR) [6], different speed rolling (DSR) [9], equal channel angular pressing (ECAP) [10, 11], high-temperature rolling [12], have been performed on Mg alloys to modify the basal texture. Moreover, our previous studies indicated that AZ31 sheets after six passes repeated unidirectional bending (RUB) process exhibit a RD-tilt and a weakened basal texture, and the formability is considerably increased at room temperature [13]. However, many methods are rather difficult to apply in industrial application due to their requirement of several passes and annealing between passes for a favorable texture.

Received date: January 03, 2019
Foundation item: National Key Research and Development Program of China (2016YFB0301104); National Natural Science Foundation of China (51671041, 51531002); Taiyuan University of Science and Technology Scientific Research Initial Funding (20182030)
Corresponding author: Huang Guangsheng, Ph. D., Professor, State Key Laboratory of Mechanical Transmission, College of Materials Science and Engineering, Chongqing University, Chongqing 400044, P. R. China, Tel: 0086-23-65112239, E-mail: gshuang@cqu.edu.cn

Copyright © 2020, Northwest Institute for Nonferrous Metal Research. Published by Science Press. All rights reserved.

Therefore, a continuous deformation is potentially one of the more practical method.

For this reason, our previous study [14] put forward a time-efficient method of continuous bending (CB) process and indicated that the formability of AZ31 Mg alloy sheets processed by one pass CB and annealing can be significantly enhanced at room temperature. However, less attention has been devoted to the effects of accumulated strain in a single pass on microstructure and properties of Mg alloy sheets. Thus, in this work, rolled AZ31 Mg sheets were subjected to CB process with various accumulated strains through changing amount of support. The microstructure and texture evolution of AZ31 Mg alloy sheets were systematically investigated. Mechanical properties and stretch formability of the as-received and CB sheets were also examined based on the concurrent microstructure and texture evolution.

1 Experiment

The schematic diagram of continuous bending device is shown in Fig.1. The commercial as-rolled AZ31 Mg alloy sheets with a thickness of 0.6 mm were used. Then the as-received sheets were cut into the dimension of 1000 mm (RD)×100 mm (TD)×0.6 mm (ND). RD, TD and ND represent the rolling, transverse and normal directions, respectively. The sheets were bent along RD at the bending angle of 140°. The true strain of each bending introduced to the surface of sheets was calculated by the empirical equation:

$$\varepsilon=t/(2R+t) \quad (1)$$

where ε is true strain, t is thickness of the sheet, R is radius of concave surface shown in Fig.2. The value of R_1 and R_2 is 14.5 and 7.2 mm, respectively. According to the different numbers of supports in the upper die, the sheets processed by CB were named as CB-1, CB-2 and CB-3. The cumulative strains for CB-1, CB-2 and CB-3 samples were 0.08, 0.16 and 0.24, respectively. Then all the CB processed sheets were annealed at 260 ℃ for 1 h, marked as CBA samples.

Microstructure evolution was examined by optical microscopy (OM) in the RD-ND plane at different regions. The mean grain sizes of all samples were measured from the optical microstructures by linear intercept method. The (0002) pole figures of various samples were determined using an X-ray diffraction (XRD, Rigaku D/Max 2500PC).

The samples for tensile test were dog-bone shape with 40 mm in gauge length along RD and 8 mm× 0.6 mm in cross section. Uniaxial tensile tests were performed on a CMT6305-300kN electronic universal testing machine. Each tension test was repeated three times to get representative results. Fracture surfaces of tensile samples were

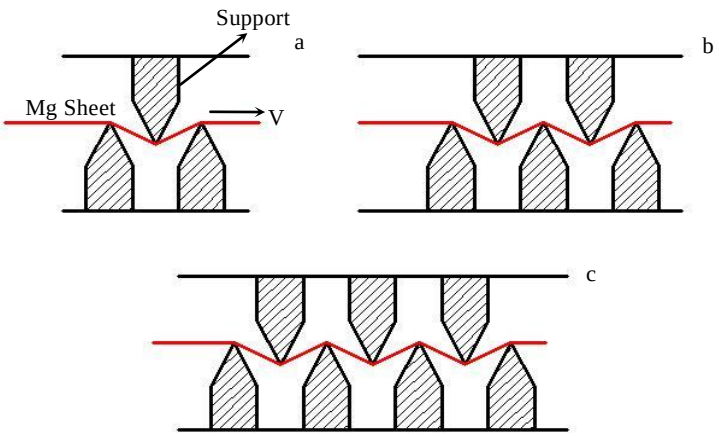

Fig.1 Schematic diagram of a continuous bending device: (a) CB-1, (b) CB-2 and (c) CB-3

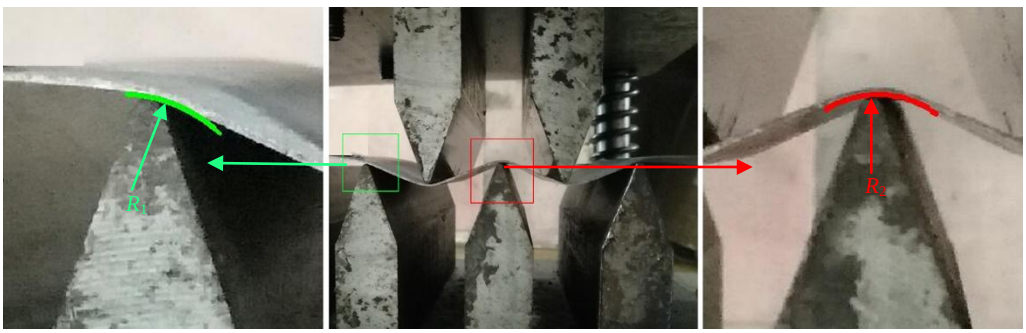

Fig.2 Experimental setup of CB process

observed in detail by scanning electron microscopy (SEM, TESCAN VEGA 3). Lankford values ($r=\omega_w/\omega_t$, where ω_w and ω_t represent width and thickness strains, respectively) were obtained from the tensile samples deformed to a tensile direction strain of 10%. The hardening index *n*-values were got from the uniform plastic deformation region of the tensile stress-strain curves.

Erichsen tests were conducted to evaluate the formability of various samples at room temperature. Rectangular blanks with dimension of 50 mm×50 mm (width×length) were cut from the as-received and CBA sheets. The Erichsen tests were carried out using a hemispherical punch with a diameter of 20 mm. The punch speed and the blank holder force were set at 3 mm/min and 10 kN, respectively.

2 Results and Discussion

2.1 Microstructure and texture evolution

The optical microstructure and (0002) pole figure of the as-received sample are shown in Fig.3. It can be seen from the microstructure that the as-received sample exhibits a fine-grain microstructure with an average grain size of 5.8 μm. The pole figure shows that the as-received sample exhibits a typical basal texture with the (0002) basal planes aligned almost parallel to the sheet surface.

Fig.4 shows the optical microstructures at different regions during CB-2 process. In the I, II and III regions, the samples are taken from the sheet at strains (ε) of 0.06, 0.10 and 0.16, respectively. The concave and convex of the sheet in I region are defined as upper and lower surface, respectively. As shown in Fig.4, there are no twins observed in all microstructures in the surface part, which is opposite to the previous study [15, 16]. It was reported that grains in concave and convex regions are under compressive and tensile stresses during V-bending, respectively. $\{10\bar{1}2\}$ extension twins are activated by the compressive stress in the concave region, while prismatic slip dominates the deformation in convex region. For magnesium alloys, twinning activity is very sensitive to grain size. Twinning activity decreases with decreasing the grain size and can even be stopped at sufficiently lower grain sizes [17-19]. Thus, the fine-grain microstructure of AZ31 Mg alloy sheets in this work may result in the absence of twins during CB. In order to coordinate the deformation, pyramidal slips need to be activated. This is because $\{10\bar{1}2\}$ twinning and pyramidal <*c*+*a*> slip are the only systems that provide deformation in the *c*-axis direction and compete with each other. And there is a transition from twinning to slip dominated deformation with decrease in grain size [17, 20]. Therefore, it is suggested that pyramidal <*c*+*a*> slip dominates the deformation in concave region, while prismatic slip dominates the deformation in convex region. Due to the up-down bending, prismatic slip and pyramidal <*c*+*a*> slip alternately dominates the deformation.

The optical microstructures and (0002) pole figures of CBA samples are illustrated in Fig.5. As shown in Fig.5a~5c, abnormal grain growth is observed in the surface part. The depth *h* of coarse-grained layer increases with the increase of accumulated strain in CB process. The abnormal grain growth may be owing to the heterogeneity deformation between surface and center part. During V-bending, AZ31 Mg alloy sheets bear varying strains throughout the sheet thickness [16]. The surface part has larger strain than the center, leading to larger driving force for grain growth during annealing [21]. Thus, the grains near the surface grow obviously and there is no significant difference in the center.

Fig.5d~5f show the (0002) pole figures of CBA samples measured by XRD. As shown in Fig.5d and 5e, the CBA-1 and CBA-2 samples still exhibit a typical basal texture with the basal poles inclined towards RD. The pole figure of CBA-2 sample exhibits a larger inclined angle than CBA-1 sample, which may be attributed to the larger accumulated strains induced by CB process. The CBA-3 sample is characterized by (0002) texture with a double-peak distribution. The spilt and rotation of basal poles are likely to be related to the occurrence of pyramidal <*c*+*a*> slip. Due to the inclination of basal poles, the dislocations with a <*c*> Burgers vector component are needed to accommodate the strain in the normal direction. For the suppression of twinning during bending, the <*c*+*a*> pyramidal slip is needed and also favorably oriented for the chosen deformation geometry [22]. Previous studies [23-25] also indicated that the activity of <*c*+*a*> slip leads to an increase

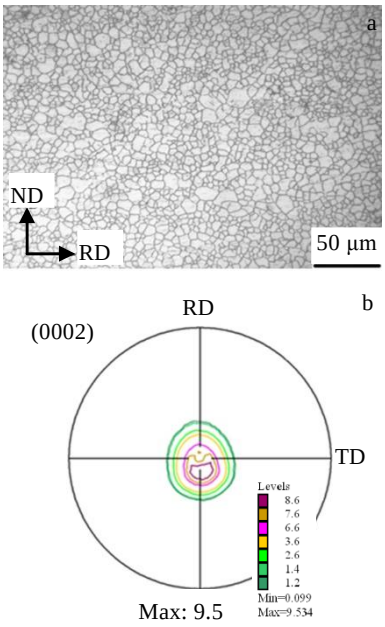

Fig.3 OM image (a) and (0002) pole figure (b) of as-received sample

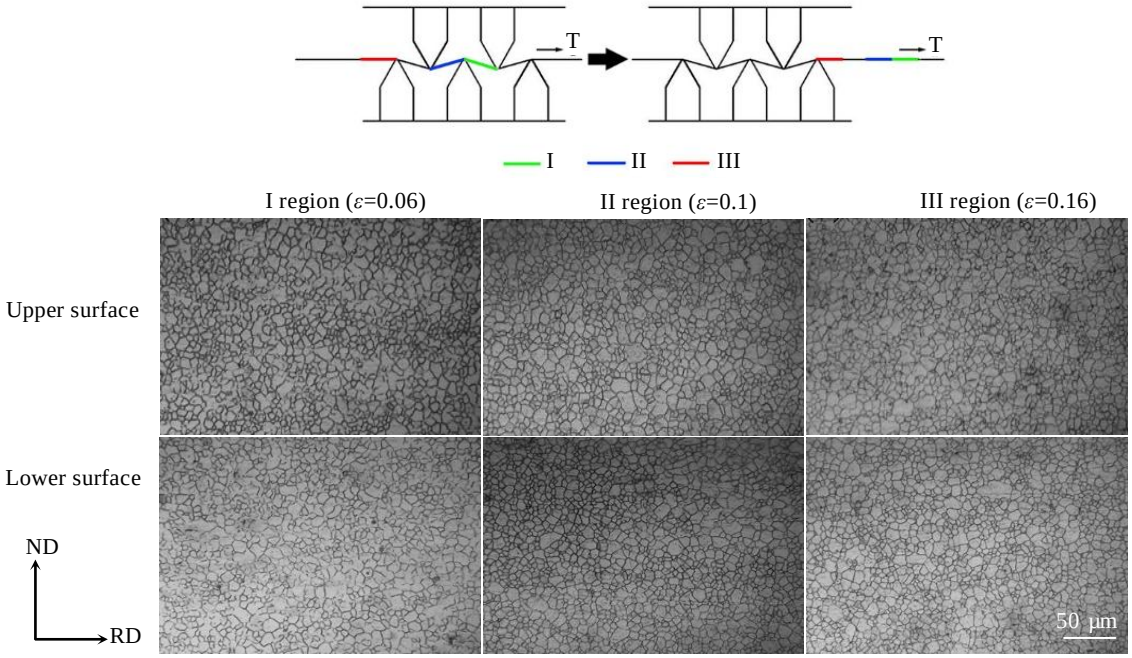

Fig.4 OM images of different regions with different strains during CB-2 process

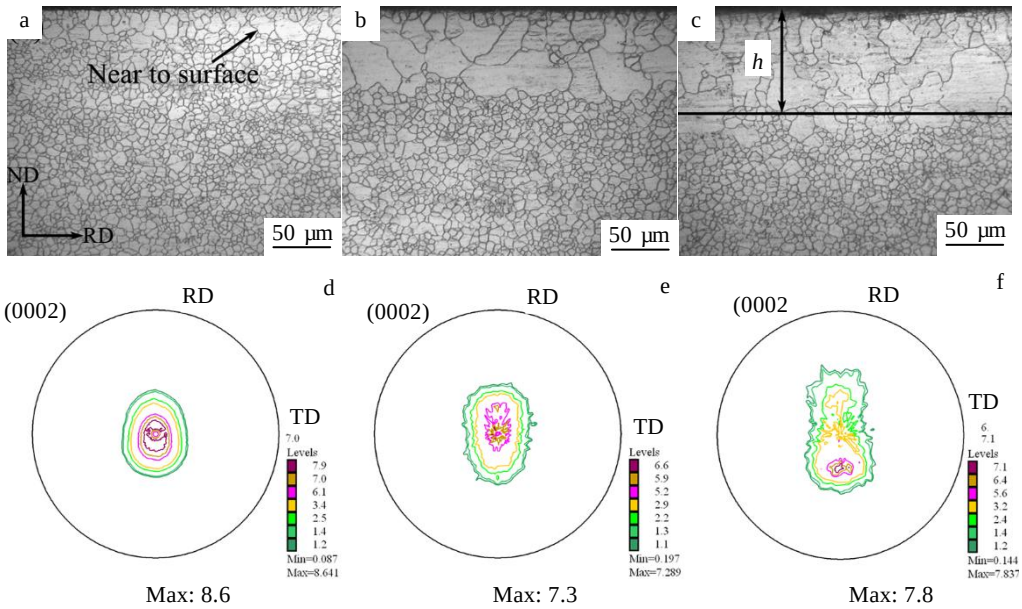

Fig.5 OM images (a~c) and (0002) pole figures (d~f) of CBA-1 (a, d), CBA-2 (b, e) and CBA-3 (c, f) samples

tendency of basal poles, rotating from ND towards RD. Compared with as-received sample, the basal texture intensity of CBA samples is gradually reduced with increasing the accumulated strain from the CB process.

2.2 Mechanical properties and formability

True stress-strain curves of as-received and various CBA samples are presented in Fig.6. The corresponding mechanical properties including yield strength (YS), ultimate strength (UTS) and failure elongation (FE) are summarized in Table 1, and *r*-values and hardening index *n*-values are also included. Compared with as-received sample, CBA samples exhibit a decrease trend in YS. It is well known that <*a*> basal slip has a great influence on the yield strength due to its lowest critical resolved shear stress (CRSS) [26]. The larger the Schmid factor of basal slip systems, the more easily the basal slip is activated during tension, which is beneficial to the decrease in YS. Thus, due to the basal texture randomizing and weakening behavior, the Schmid factor of basal <*a*> slip increases, leading to the decrease in YS. In addition, the FE of CBA samples

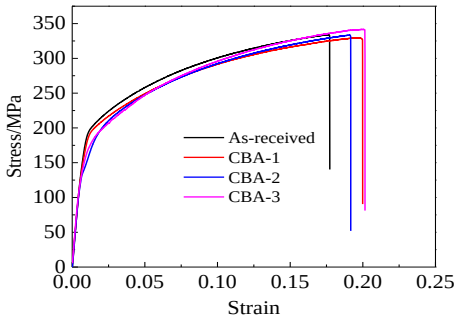

Fig.6 True stress-strain curves of various samples

Table 1 Mechanical properties of various samples

Sample	YS/MPa	UTS/MPa	FE/%	*r*	*n*
As-received	183	334	16.5	2.98	0.23
CBA-1	169	336	19.0	2.85	0.24
CBA-2	140	328	18.2	2.13	0.26
CBA-3	148	341	19.2	1.97	0.27

increases from 16.5% to 19.0%, 18.2% and 19.2%. The SEM images of tensile fracture surface of as-received and CBA samples are shown in Fig.7. It can be seen from Fig.7a that there are many cleavage planes, tear ridges and a small amount of shallower dimples. The fracture surface belonging to the brittle mode shows the quasi-cleavage pattern. For AZ31 magnesium alloy with the hcp structure, restricted slip systems can be activated during tension, leading to the poor ductility at room temperature. After CB process followed by annealing, a large number of dimples appear on the fracture surface, indicating the ductile fracture mode. The enhanced ductility may be ascribed to the easy activity of basal <*a*> slip, resulted from the randomized and weakened basal texture. The easy activation of basal slip may restrict the occurrence of $\{10\bar{1}1\}$ twinning, which will cause localized deformation and early failure [27].

The Erichsen value (IE) of various samples is summarized in Fig.8. For as-received sample, the strong basal texture suggests that most grains are in a hard orientation and it is difficult to activate the basal <*a*> slip, leading to stress localization and early failure [25]. Furthermore, the samples with strong basal texture exhibit a great plastic anisotropy, which induces a poor deformation capability of sheet thinning during stretch forming [28]. This results in a low ductility and a poor formability with the IE of 2.3 mm at room temperature. Compared with as-received sample, the CBA samples exhibit higher IEs of 3.8 mm (increased by 60.9%), 4.5 mm (increased by 95.7%) and 4.9 mm (increased by 113.0%). The improved formability of CBA samples can be attributed to the RD-tilt and weakened basal texture, which result in a smaller *r*-value and larger

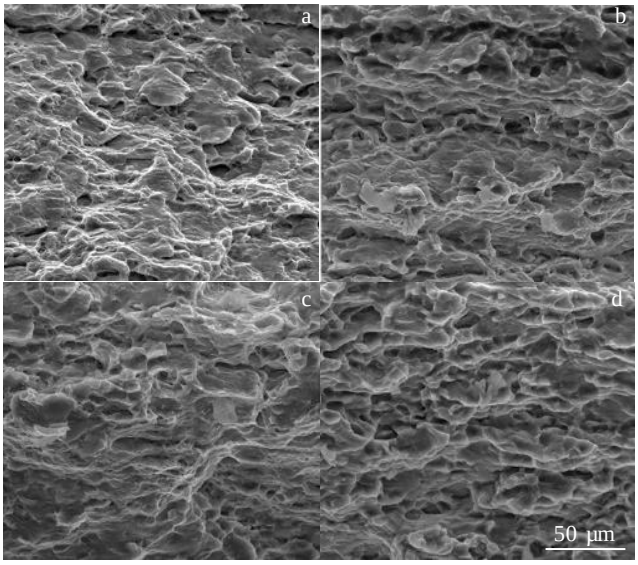

Fig.7 SEM images of tensile fracture surface of as-received (a), CBA-1 (b), CBA-2 (c) and CBA-3 (c) samples

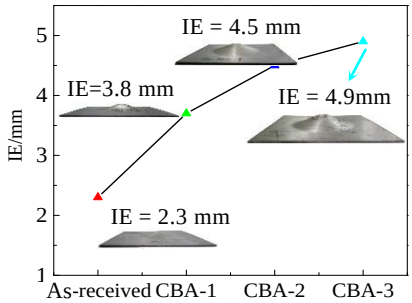

Fig.8 Erichsen value (IE) of different samples

n-value, as shown in Table 1. Previous studies[26, 28] indicated that prismatic <*a*> slip dominates the width strain and pyramidal <*c*+*a*> slips with the largest CRSS generate the thickness strain. This leads to a high *r*-value in strong basal texture magnesium alloys. For the weak basal texture with well-tilted *c*-axes, the basal <*a*> slip with the lowest CRSS greatly contributes to the thickness strain, which leads to a decrease in the *r*-value. This helps to enhance the deformation capability of sheet thinning during sheet forming. In addition, the larger *n*-value owing to the RD-tilt basal texture may be responsible for the enhanced formability. Kang et al [29] reported that magnesium alloys with a random texture will have a large work-hardening capacity since a large number of grains will be favorably oriented for deformation. The larger *n*-value leads to a low sensitivity to strain localization in the formation of necking, which contributes to the enhancement of formability [12]. Therefore, the improvement in stretch formability can be attributed to the smaller *r*-values and larger *n*-values related to the weakened and RD-tilt basal texture.

3 Conclusions

1) AZ31 Mg alloy sheets after different strain CB process exhibit a twin-free microstructure. After annealing, abnormal grain growth occurs in the surface part and the depth of coarse-grained layer increases with increasing the accumulated strain. A weakened basal texture can be obtained with the basal poles inclined to RD after CB process followed by annealing.

2) The sheets processed by CB and annealing treatment exhibit lower yield strengths (148 MPa vs 183 MPa) and higher fracture elongation (19.2% vs 16.5%), which is mainly attributed to the texture evolution.

3) Due to the randomized and weakened basal texture, AZ31 Mg alloy sheets processed by CB and annealing treatment exhibit smaller *r*-values and larger *n*-values, and the formability can be significantly enhanced.

References

1 Aatthisugan I, Razal Rose A, Selwyn Jebadurai D. *Journal of Magnesium and Alloys*[J], 2017, 5(1): 20
2 Wu Y, Yan H, Chen J *et al*. *Materials Science and Technology*[J], 2013, 29(1): 54
3 Chelliah Nagaraj M, Kumar Ram, Singh Harpreet *et al*. *Journal of Magnesium and Alloys*[J], 2017, 5(1): 35
4 You S, Huang Y, Kainer K U *et al*. *Journal of Magnesium and Alloys*[J], 2017, 5(3): 239
5 Yang Qingshan, Yu Zujian, Dai Qingwei *et al*. *Materials Research*[J], 2016, 19(2): 322
6 Zhang Hua, Huang Guangsheng, Wang Lifei *et al*. *Journal of Alloys and Compounds*[J], 2013, 575: 408
7 Huo Qinghua, Yang Xuyue, Ma Jijun *et al*. *Materials Characterization*[J], 2013, 79: 43
8 Griffiths D. *Materials Science and Technology*[J], 2015, 31(1): 10
9 Huang Xinsheng, Suzuki Kazutaka, Watazu Akira *et al*. *Journal of Alloys and Compounds*[J], 2009, 470(1-2): 263
10 Suh J, Victoria-Hernandez J, Letzig D *et al*. *Journal of Materials Processing Technology*[J], 2015, 217: 286
11 Suh J, Victoria-Hernández J, Letzig D *et al*. *Materials Science and Engineering A*[J], 2016, 669: 159
12 Huang Xinsheng, Suzuki Kazutaka, Chino Yasumasa *et al*. *Journal of Alloys and Compounds*[J], 2015, 632: 94
13 Song Bo, Huang Guangsheng, Li Hongcheng *et al*. *Journal of Alloys and Compounds*[J], 2010, 489(2): 475
14 Han Tingzhuang, Huang Guangsheng, Wang Yougen *et al*. *Transactions of Nonferrous Metals Society of China*[J], 2016, 26(8): 2043
15 Huang Guangsheng, Wang Lifei, Zhang Hua *et al*. *Materials Letters*[J], 2013, 98: 47
16 Habibnejad-Korayem M, Jain M K, Mishra R K. *Materials Science and Engineering A*[J], 2015, 648: 371
17 Barnett M, Keshavarz Z, Beer A *et al*. *Acta Materialia*[J], 2004, 52(17): 5093
18 Shi B Q, Chen R S, Ke W. *Journal of Magnesium and Alloys*[J], 2013, 1(3): 210
19 Tsai M S, Chang C P. *Materials Science and Technology*[J], 2013, 29(6): 759
20 Wang Huiyuan, Xue Ensong, Xiao Wei *et al*. *Materials Science and Engineering A*[J], 2011, 528(29-30): 8790
21 Zhang Hua, Huang Guangsheng, Song Bo *et al*. *Transactions of Nonferrous Metals Society of China*[J], 2011, 21(4): 844
22 Liu Zhiyi, Huang Tiantian, Liu Wenjuan *et al*. *Transactions of Nonferrous Metals Society of China*[J], 2016, 26(2): 378
23 Wang J, Zhang X, Lu X *et al*. *Journal of Magnesium and Alloys*[J], 2016, 4(3): 207
24 Zhou Tao, Zhao Yang, Hu Dong *et al*. *Journal of Alloys and Compounds*[J], 2015, 650: 436
25 Zhang Hua, Cheng Weili, Fan Jianfeng *et al*. *Materials Science and Engineering A*[J], 2015, 637: 243
26 Huang Xinsheng, Suzuki Kazutaka, Saito Naobumi, *Scripta Materialia*[J], 2009, 60(8): 651
27 Yan H, Chen R S, Han E H. *Materials Characterization*[J], 2011, 62(3): 321
28 Zhang Hua, Huang Guangsheng, Wang Lifei *et al*. *Scripta Materialia*[J], 2013, 69(1): 49
29 Kang D H, Kim D W, Kim S *et al*. *Scripta Materialia*[J], 2009, 61(7): 768

AZ31 镁合金薄板经不同累积应变的连续弯曲变形后的显微组织与成形性能

韩廷状[1]，黄光胜[2]，王利飞[3]，蒋 斌[2]，王冠刚[2]，汤爱涛[2]，潘复生[2]

（1. 太原科技大学 重型机械教育部工程研究中心，山西 太原 030024）

（2. 重庆大学 机械传动国家重点实验室，重庆 400044）

（3. 太原理工大学，山西 太原 030024）

摘 要：对 AZ31 镁合金板材进行不同累积应变的连续弯曲变形及退火处理，随后对显微组织与力学性能的变化进行了研究。结果表明：经不同累积应变的连续弯曲变形后，镁合金板材的显微组织中没有发现孪晶，退火后，板材表层的晶粒异常长大，粗晶层的厚度随着累积应变的增加而增加，并且镁合金板材的织构朝 RD 方向偏转，偏转角度随累积应变的增加而增大；与原始板材相比，连续弯曲变形及退火处理使镁合金板材呈现出较好的室温成形性能（杯突值由 2.3 mm 提高到 4.9 mm，提高了~113%），这主要归因于基面织构的改善使镁合金板材的 *r* 值减小与 *n* 值增大。

关键字：镁合金；连续弯曲；显微组织；织构；力学性能；成形性能

作者简介：韩廷状，男，1989 年生，博士，讲师，太原科技大学材料科学与工程学院，山西 太原 030024，E-mail: htzhhbhs@163.com